ENERGY DISSIPATION AND BUBBLES GENERATION IN A GRAVITATIONAL GAS SEPARATOR

Luis Enrique Ortiz Vidal*,[1], Oscar Mauricio Hernandez Rodriguez*,[2] , Valdir Estevam°, Divonsir Lopes[§]

* Department of Mechanical Engineering, Engineering School of São Carlos, University of São Paulo (USP), Av. Trabalhador São-carlense, 400, São Carlos-SP, Brasil, Email: [1]leortiz@sc.usp.br, [2]oscarmhr@sc.usp.br
° Exploration and Production – Corporate, PETROBRAS, Email: vestevam@petrobras.com.br
[§] E&P/UN-Rio/ST/EE, PETROBRAS, Email: divonsir@petrobras.com.br

ABSTRACT

Different types of gravitational gas separators have been proposed to avoid failures in the submergible centrifugal pump (SCP) systems caused by the excess of free gas in the suction of the pump. Recently, a new and elucidating model for the inverted-shroud gas separator has been reported in the literature. That model describes the inverted-shroud separator phenomenology and it is proposed a methodology for the prediction of the total gas separation as a function of the two-phase turbulent kinetic energy dissipation into the separator. However, the energy dissipation length parameter (L_{dis}) is considered constant. The main goals of this study are the development and experimental validation of a correlation for L_{dis} that ensures the total gas separation. New data were collected in an inclined inverted-shroud separator of diameter 65 mm and length 7.5 m at 15 and 45 degrees from the horizontal. Air and water at near atmospheric pressure constituted the gas and liquid phases. The experimental work determined the function of L_{dis} with inclination angle, liquid flow rate and liquid viscosity. The results show that the proposed correlation can be applied for the optimized design of the proposed inclined inverted-shroud separator.

INTRODUCTION

Failures in the submergible centrifugal pump (SCP) are caused by high quantities of free gas in the suction of the pump. This problem is avoided by employing gas separators of centrifugal, helical or gravitational types.

Centrifugal separators have the problem of high maintenance costs due to the moving parts, although they present better separation efficiencies. Fixed helical separators overcome the moving-part problem, but the helix reduces the cross-sectional area of the annular channel. Available data show that centrifugal and helical separators have similar separation efficiencies [1-3].

The literature also repots a gravitational gas separator with annular geometry known as inverted-shroud separator [4-5]. Those authors show that it can reach separation efficiencies similar to those achieved by centrifugal and helical separators. Unfortunately the information available on inverted-shroud separators is quite scanty.

Although Vidal *et al.* [4] present an elucidating phenomenological model for total gas separation based on the two-phase turbulent kinetic energy dissipation, they do not offer any expression for the energy dissipation length parameter (L_{dis}).

The main goals of the present study are the development and validation of a correlation for L_{dis} that ensures the total gas separation for the Vidal *et al.*'s model.

REPORTED MODELLING

Vidal *et al.* (2009) [4] reported a new phenomenological model for gravitational gas separation in an inclined annular channel whose geometry is similar to the present inverted-shroud separator. The researchers noted that when the separator is installed in an inclined angle it has the potential to convert a downstream, vertical and chaotic flow into a free-surface flow, and the incorporation of gas during the impact between the liquid phase and liquid interface, which happens at the inner-annular level (*IAL*, Fig.1), is reduced.

The researchers showed that the phenomenology of the inverted-shroud separator is essentially as function of four types of flows (Fig.1): an upward two-phase annular-channel flow (flow type A) is observed when the two-phase mixture flows through the outer annular channel; at the shroud inlet occurs segregation of the gas and liquid phases, thus a free-surface annular-channel liquid flow driven by gravity is presented (flow type B),*i.e.*, the liquid phase flows through the inverted-shroud; when the free-surface flow impacts on the inner-annular liquid level (*IAL*) an aeration process occurs, this type of flow was called transition annular-channel flow by the researchers (flow type C); if the inverted-shroud separator works properly the production pipe has only single-phase liquid flow to deal with (flow type D).

The model was qualitatively compared with data from the literature [5], with good agreement. The Vidal *et al.*' model explains physically the results obtained by Rondy *et al.* [5], *i.e.*: the separation efficiency increases with increasing the liquid viscosity; the separation efficiency increases with increasing the liquid flow rate; and the separation efficiency decreases with increasing the gas flow rate.

Features of the Phenomenological Modelling

The reported model [4] proposed a total gas separation criterion based on the prediction of the *IAL* position: there is a specific position of *IAL* for which there is a minimum length a_{IAL} that ensures the total gravitational separation of all bubbles generated in the type C flow (see Fig.1).

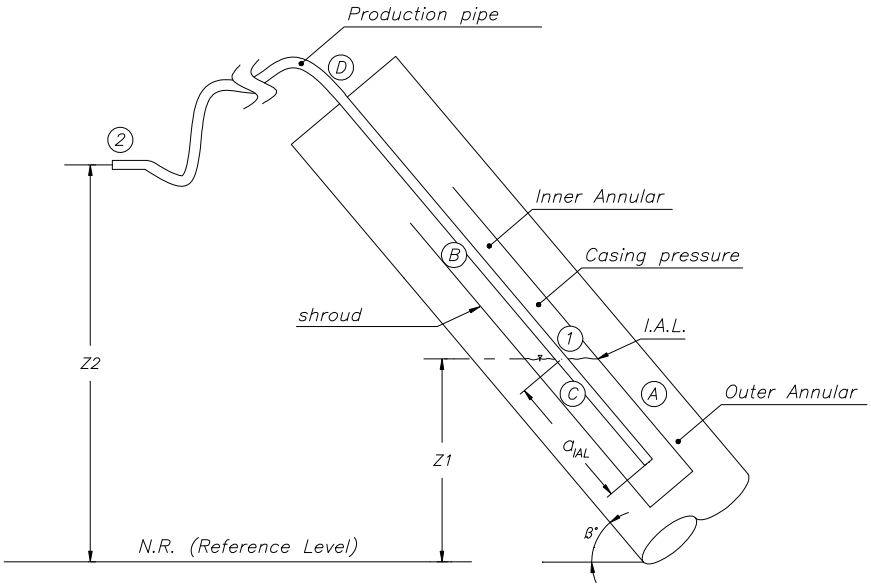

Figure 1. Schematic description of the phenomenology of inverted-shroud separator presented by Vidal *et al.* (2009) [4]. The points 1 and 2 indicate the path of the liquid from the inner-annular level (IAL) to the the production pipe outlet, respectively. The letters represent flow types.

It is supposed that in the transition annular-channel flow (type C, Fig.1) bubbles are generated due to the turbulent kinetic energy dissipation. These bubbles are subjected to turbulence, gravity, buoyancy and drag forces.

The length a_{IAL} that ensures the total separation of the bubbles can be expressed by

$$a_{AIL} \geq a_{dev} + a_{Stokes} \tag{1}$$

where a_{dev} and a_{Stokes} stand for development length of the velocity profile and length of the parabolic path of the bubbles in the inner-annular channel, respectively, given by [6-8]:

$$a_{Stokes} = V_{ai}\left(\frac{(\pi/2)d_{ii}}{V_{ter}}\right) \tag{2}$$

$$a_{dev} = 4.4\,\mathrm{Re}_{ai}^{1/6}\,d_{ai} \tag{3}$$

where V_{ai} and V_{ter} are the inner-annular channel and terminal velocity, respectively.

From the equation of conservation of mass for steady state and fully-developed flow it is determined the inner-annular channel velocity as follows [6; 8-9]:

$$Q_p = A_{sl}V_{sl} = A_{ai}V_{ai} = A_{tp}V_{tp} \tag{4}$$

$$V_{ai} = \frac{Q_p}{A_{ai}} \tag{5}$$

According to Stokes' law, the terminal velocity is as follows [6-7]:

$$V_{ter} = \frac{(\rho_w - \rho_a)g{d_b}^2}{18\mu_w} \tag{6}$$

where d_b is the bubble diameter. This diameter is estimated from the balance between surface tension and shear stress forces [7; 10-11]:

$$d_b = 1{,}15\left(\frac{\sigma}{\rho_w}\right)^{0,6} {E_{dis}}^{-0,4} \tag{7}$$

where E represents the energy dissipation rate per unit of mass and can be expressed by:

$$E_{dis} = \frac{1}{2}\frac{V_{sl}^3}{L_{dis}} \tag{8}$$

The free-surface liquid velocity (V_{sl}) is expressed by [6; 9; 12]:

$$V_{sl} = \sqrt{\frac{2gD_{sl}Sin(\beta)}{f_{sl}}} \tag{9}$$

where D_{sl} is the hydraulic diameter of the free-surface flow, f_{sl} is the Darcy's friction factor for free-surface flow and β is the shroud inclination angle.

Details for the calculation of f_{sl} , and D_{sl} can be found in [4; 8; 13-15].

ENERGY DISSIPATION LENGTH

Deduction of L_{dis}

Considering steady state, the kinetic energy per unity mass of the free-surface liquid flow before impacting on the inner-annular liquid level (*IAL*) can be represented as follows

$$ec = \frac{1}{2} V_{sl}^2 \tag{10}$$

We suppose that all kinetic energy is dissipated in the transition annular-channel flow (type C, Fig.1). Therefore, the energy dissipation rate per unit of mass can be given by

$$E_{dis} = \frac{\dot{m}}{M} ec = \frac{\dot{m}}{2M} V_{sl}^2 \tag{11}$$

where $\dot{m}$ is the mass flow rate of the free-surface flow and M is a generic mass of liquid related to the amount of energy dissipated within a certain length.

The factor $\dot{m} / M$ of Eq.(11) can be expressed by

$$\frac{\dot{m}}{M} = \frac{\rho_w Q_p}{\rho_w \forall} = \frac{\rho_w A_{sl} V_{sl}}{\rho_w A_{sl} L_{dis}} \tag{12}$$

Reducing and substituting Eq. (12) into Eq. (11) one obtains:

$$L_{dis} = \frac{1}{2} \frac{V_{sl}^3}{E_{dis}} \tag{13}$$

where the parameter L_{dis} is the energy dissipation length of a generic liquid mass and it is related the two-phase turbulent kinetic energy dissipation.

Correlation for L_{dis}

A correlation for L_{dis} based on the phenomenology described above as a function of the liquid flow rate (Q_p), liquid viscosity (μ_w) and inclination angle (β) was developed.

Based on the experimental observation:

$$L_{dis} \propto \mu_w, \beta, \frac{1}{Q_p} \tag{14}$$

Then, the following empirical correlation for L_{dis} is proposed:

$$L_{dis} = c_1 \left(\frac{Q_o}{Q_p} \right)^{n\sqrt{sin\beta}} \tag{15}$$

where c_1 and n are constants to be adjusted and the liquid viscosity is implicitly taken into account in the Q_o parameter. It represents the critical liquid flow rate related to transition from laminar to turbulent flow in the inner-annular channel,

$$Q_o = \mathrm{Re}_{tr} \frac{\mu_w A_{ai}}{\rho_w D_{ai}}, \mathrm{Re}_{tr} = 2100 \tag{16}$$

where D_{ai} and A_{ai} are the hydraulic diameter and cross-sectional area of the inner-annular channel, respectively. It should be noted that Eq.(15) is valid for turbulent annular-channel flow.

EXPERIMENTAL WORK AND FACILITIES

The experimental work was performed at air-water test loop of the Thermal-Fluids Engineering Laboratory (LETeF) of the Engineering School of São Carlos (USP). The collected data were used to adjust constants c_1 and n of Eq.(15). Fig.3 shows a schematic representation of the test loop. The components and measurement instruments are designated by letters and numbers and are listed in Tab. 1 and 2, respectively.

Table 1. Air-water test loop components.

Letter	Component
A	Air Compressor
B	Cooling and filtering system
C	Air tank
D	Air regulating valve
E	Globe valve Ø1 1/2”
F	Water Tank
G	Globe valve Ø1 1/2”
H	Globe valve Ø1 1/2”
I	Water screw pump
J	Frequency shifter
K	Globe valve Ø1 1/2”
L	Globe valve Ø1 1/2”
M	Air/Water mixer
N	Inclined structure system
O	Test sections - 10,5 m.
P	Air Pressure regulator valve
Q	Air/Water separator tank

Water from the tank F flows through pump I and its flow rate was measured by the positive-displacement flow meter 4. Water is mixed with air in the mixer and the two-phase mixture flows through the test section. The air flow rate was measured upstream and downstream by identical positive-displacement flow meters 1 and 9, respectively. The mixture was collected and separated by gravity in tank Q.

The test section is made of tree concentric tubes. The outer (casing) and inner (shroud) tubes are made of glass. There is also an innermost pipe (production pipe) made of PVC (see Fig.1). The total test-section length was 10.5 m and was assembled in sections of 1.5 m by means of PVC flanges. The external diameters of the outer tube and shroud were 115 and 75 mm, respectively, and both had wall thicknesses of 5 mm. The external and internal diameters of the production pipe were 20 and 17 mm, respectively.

Experiments were conducted in the test section at 15 and 45 degrees from the horizontal. Air and water at near atmospheric pressure constituted the work fluids. The liquid flow rate was in the 9-26 l/min range and the average inlet gas mass flow rate was 1.18 kg/hr. Data of gas-separation efficiency were collected as a function of liquid flow rate (Q_p), inlet and outlet air mass flow rates, inclination angle and *IAL* position.

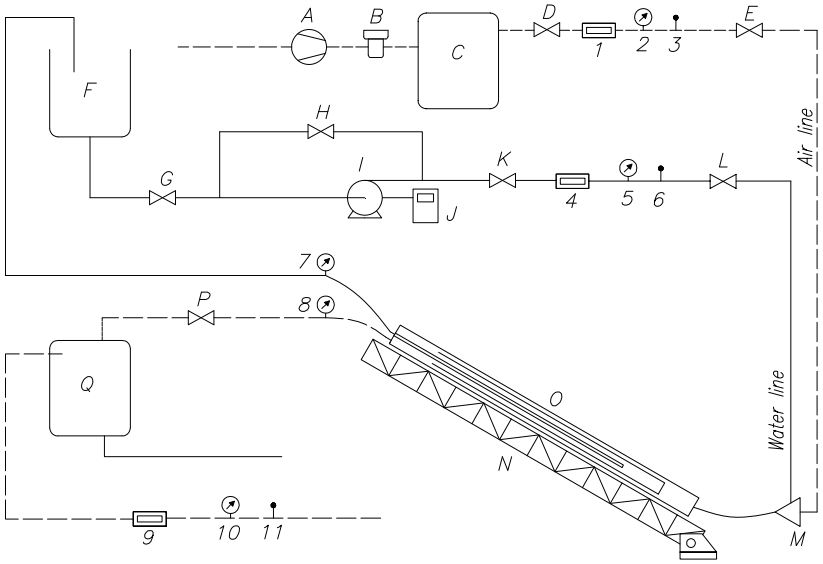

Figure 3. Air-water test loop at the Thermal-Fluids Engineering Laboratory (LETeF) of the Engineering School of São Carlos (USP). The letters and numbers represent the components and measurement instruments, respectively (refer to Tab. 1 and 2).

Table 2. Measurement instruments of test loop

Number	Component	Manufacture/model	Range	Accuracy
1	Air flowmeter	Oval Gal50	0 to 20 l/min	1%FE
2	Pressure transducer	Novus 510	0 to 5 bar	0.5% FE
3	Temperature sensor	APPA MT-520	-200 to 1372 °C	0.1%RD+1°C
4	Water flowmeter	Oval OGT	1 to 35 l/min	0.75% RD
5	Pressure transducer	Novus 510	0 to 5 bar	0.5% FE
6	Temperature sensor	APPA MT-520	-200 to 1372 °C	0.1%RD+1°C
7	Pressure transducer	Novus 691	-1 to 1 bar	0.3%FE
8	Pressure transducer	Novus 510	0 to 5 bar	0.5% FE
9	Air flowmeter	Oval Gal50	0 to 20 l/min	1%FE
10	Mercury barometer	Princo 453	647 to 830 mm Hg	0.5 mm Hg
11	Mercury thermometer	Princo 453	15 to 50 °C	0.5 °C

RESULTS AND DISCUSSION

The Vidal *et al.*'s model [4] was implemented in Mathematica® and applied to simulate the flow and geometric conditions carried out in the LETeF's experimental facilities.

First, the effect of c_1 on a_{IAL} were evaluated assuming that $n = 0$. Figures 4 and 5 show the results for 15 and 45 degree of inclination, respectively. It was observed that c_1 has little influence on a_{AIL} and consequently on L_{dis}. On the other hand, bubbles were seen to behave in a high turbulent manner until about 10 cm downstream the I.A.L (Fig. 1, with would suggest that the turbulent kinetic energy dissipation would occur mainly within that distance downstream. For these reasons, a value of 0.1 m was chosen for c_1.

The experimental adjustment of the L_{dis} correlation (Eq. 17) is expressed by

$$L_{dis} = 0.1\left(\frac{0.000142}{Q_p}\right)^{n\sqrt{\sin\beta}} \tag{17}$$

where L_{dis} is given in meters.

Figures 6 and 7 show comparisons between experimental a_{AIL} versus Q_p data collected in this work and model predictions for 15 and 45 degrees of inclination, respectively. Three different curves of predicted 100% gas-separation efficiency are plotted as a function of the fitting parameter n. The areas above and under the curves can be seen as regions of predicted efficiencies of 100% and less than 100%, respectively. Data of 100% and less than 100% of gas-separation efficiency are represented by the triangular and square dots, respectively. Experiments showed that $n \geq 4.5$, Eq.(17), ensures a reliable prediction of total gas separation for the tested cases.

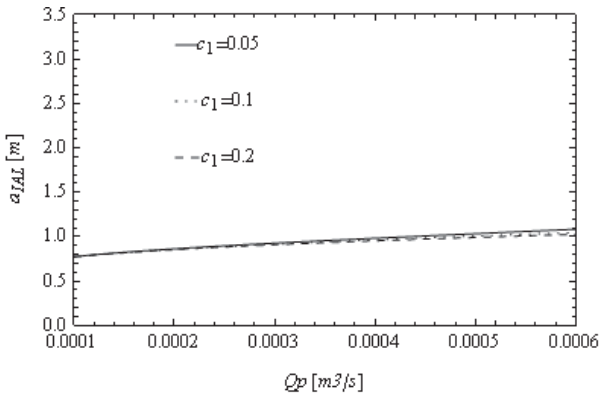

Figure 4. Influence of c_1 on a_{IAL} for $\beta = 15°$ ($\eta = 100\%$, $n = 0$)

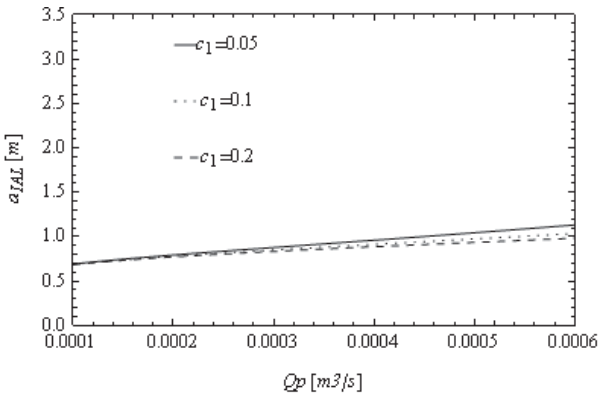

Figure 5. Influence of c_1 on a_{IAL} for $\beta = 45°$ ($\eta = 100\%$, $n = 0$)

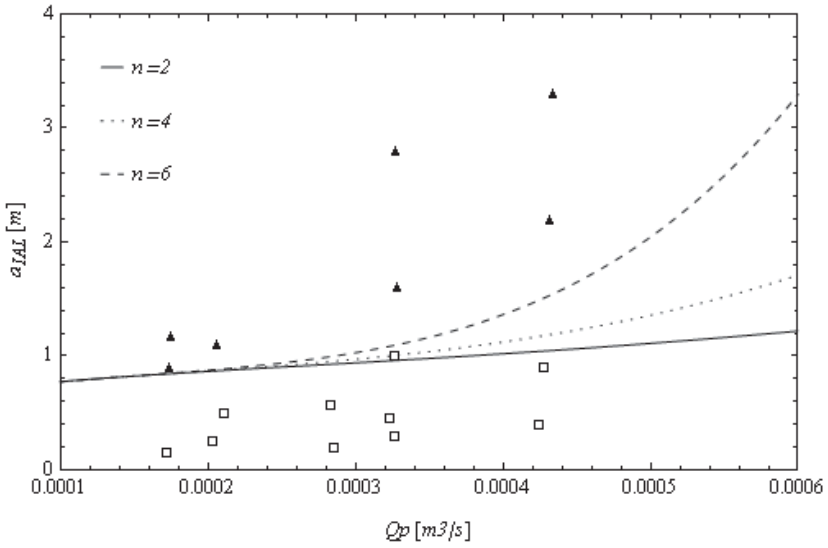

Figure 6. *IAL* length as a function of liquid flow rate. Experimental (dots) and predicted (curves) separation efficiencies for β = 15°. The lines represent 100% efficiency and show the influence of parameter n of the proposed correlation. The triangular dots represent efficiencies of 100% and the square dots efficiencies lower than 100%; n = 4 showed the best agreement.

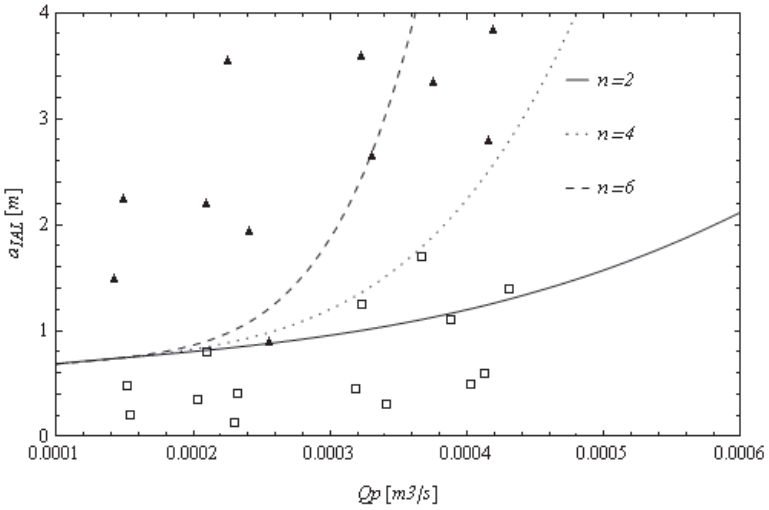

Figure 7. *IAL* length as a function of liquid flow rate. Experimental (dots) and predicted (curves) separation efficiencies for β = 45°. The lines represent 100% efficiency and show the influence of parameter n of the proposed correlation. The triangular dots represent efficiencies of 100% and the square dots efficiencies lower than 100%; n = 4 showed the best agreement

CONCLUSIONS

A new empirical correlation for the prediction of the energy dissipation length associated with the two-phase turbulent kinetic energy dissipation for in inverted-shroud separator has been presented. The correlation was based on a model found in the literature and manages to include the liquid physical properties, separator geometry, liquid flow rate and inclination angle. New data of gas-separation efficiency as function of liquid flow rate, gas mass flow rate for 15 and 45 degrees were collected. The model predictions was compared with the new experimental data and the agreement was quite good.

ACKNOWLEDGEMENTS

The authors are grateful to PETROBRAS for supporting the experimental work. L.E.O. Vidal is grateful to CAPES (Coordenação de Aperfeiçoamento de Pessoal de Nível Superior) for the scholarship.

REFERÊNCIAS

[1] F.J.S. Alhanati *et al.*, A simple model for the efficiency of rotary separators. In: *69 SPE ANNUAL TECHNICAL CONFERENCE EXHIBITION*, New Orleans, LA, USA, 1994.

[2] A.F. Harun *et al.*, A simple model to predict natural gas separation efficiency in pumped wells. In: *SPE ANNUAL TECHNICAL CONFERENCE AND EXHIBITION*, Dallas, TX, USA, 2000.

[3] R.d.O. Souza *et al.*, Separador de gás de fundo de poço de alta eficiência. In: *1 Seminario de elevación artificial, escoamento e medição*, Rio de Janeiro, Brasil, 2003.

[4] L.E.O. Vidal *et al.*, Modelo para la eficiencia de separación de gas en un ducto anular inclinado. In: *9 CONGRESO IBEROAMERICANO DE INGENIERÍA MECÁNICA*, Las Palmas de Gran Canaria, Islas Canarias, 2009.

[5] P. Rondy, H.J. Cholet and I. Federer, Optimization of heavy oil and gas pumping in horizontal wells. In: *SPE ANNUAL TECHNICAL CONFERENCE AND EXHIBITION* Houston, Texas, 1993.

[6] Y.A. Çengel and J.M. Cimbala, Mecânica dos fluidos - fundamentos e aplicações, McGraw-Hill, São Paulo, 2007.

[7] AMERICAN PETROLEUM INSTITUTE, API 421: Design and operation of oil-waters separators, Washington, 1990.

[8] O.M.H. Rodriguez, Mecânica dos Fluidos - Pos-Graduação. Apostila SEM5749, EESC-USP, São Carlos, SP, 2008.

[9] R.W. Fox, A.T. McDonald and P.J. Pritchard, Indrodução à mecânica dos fluidos, LTC - Livros Técnicos e Científicos Editora S.A., Rio de Janeiro, 2006.

[10] S. Kucukali and S. Cokgor, Energy concept for predicting hydraulic jump aeration efficiency, *Journal of Environmental Engineering-Asce*, v.135, n.2, p.105-107, 2009.

[11] P. Volkart, The mechanism of air bubble entrainment in self-aerated flow, *International Journal of Multiphase Flow*, v.6, n.5, p.411-423, 1980.

[12] M.C. Potter and D.C. Wiggert, Mecânica dos fluidos, Pioneira Thomson Learning, São Paulo, 2004.

[13] L.E.O. Vidal, D. Cabanillas and R. Fierro, Influencia del factor de fricción en el diseño de redes de tuberías: estudio de caso. In: *1 CONGRESO NACIONAL DEL AGUA*, Lima, Perú, 2009.

[14] R.G. Allen, Relating the Hazen-Williams and Darcy-Weisbach friction loss equations for pressurized irrigation, *American Society of Agricultural Engineers*, v.12, n.6, p.685-693, 1996.

[15] C.P. Blanco, T.F. Albieri and O.M.H. Rodriguez, Revisão de modelos para transições de padrão de escoamento gás-liquido em duto anular vertical e horizontal. In: *12 BRAZILIAN CONGRESS OF THERMAL ENGINEERING AND SCIENCES*, Belo Horizonte, MG, 2008.

NOMENCLATURE

A	area (m^2)
a_{IAL}	length of maximum efficiency (m)
d	diameter (m)
D	hydraulic diameter (m)
E	rate energy dissipation per mass unit (W/Kg)
e/D	relative roughness (nondimensional)
f	friction factor (nondimensional)
g	gravitational constant (m/s^2)
h_T	head loss (m)
h_w	liquid level (m)
L	pipe length (m)
L_{dis}	energy dissipation length (m)
P	pressure (Pa)
Q_p	liquid flow rate (m^3/s)
Re	Reynolds number (nondimensional)
S	perimeter (m)
V	velocity (m/s)
Z	hydrostatic height (m)
Greek letters	
μ	dynamic viscosity (Pa s)
β	inclination angle (°)
η	efficiency (nondimensional)
ρ	density (Kg/m^3)
σ	interfacial tension (N/m)
Subscripts	
1,2	input and output of control volume, respectively
a	gas
ai	inner-annular channel
b	bubble
ep	outer-production-tube
i	interface
ii	internal-shroud
tp	production-pipe
sl	free surface
w	Liquid